This paper was prepared on the Fourth International Tribology Conference ITC 2006

FRICTION INDUCED VIBRATION OF A VERY FLEXIBLE SHAFT ROTATING SLOWLY

S. KORNYEYEV[*], Y. SATO and T. NAGAMINE
Department of Mechanical Engineering, Saitama University
255 Shimo-Okubo, Sakura-ku, Saitama-shi, 338-8570 JAPAN

High frequency vibration was observed in operation of a soot-blower. To clarify its mechanism, an analysis and experiment were carried aut on a system consisting of a flexible shaft rotating slowly, on which friction acts tangentially at an intermediate position. Analytical results show that the real part of an eigenvalue does not always decrease monotonically with the order of mode. Therefore, some higher modes may appear more prominently. Large vibration is observed in experiments where real part of an eigenvalue is large.

Key words: self-excited vibration, rotating flexible shaft, friction induced vibration.

1. Introduction

A soot-blower shown in Fig.1 is used to blow off soot on tubes in a tubular heat exchanger, or a gas heater. High frequency vibrations and noises occurred in operation. A soot-blower has a long slender pipe called a lance, *8 m* long and *76 mm* in diameter, which is put slowly into a gas heater. Steam flows through the lance and is discharged at the free end to blow off soot. In operation the lance rotates about its axis at *12 rpm*. At an intermediate position the lance is supported by a support bearing, called a lance bearing (shown in Fig.1). Sato (2001) studied the mechanism of vibration.
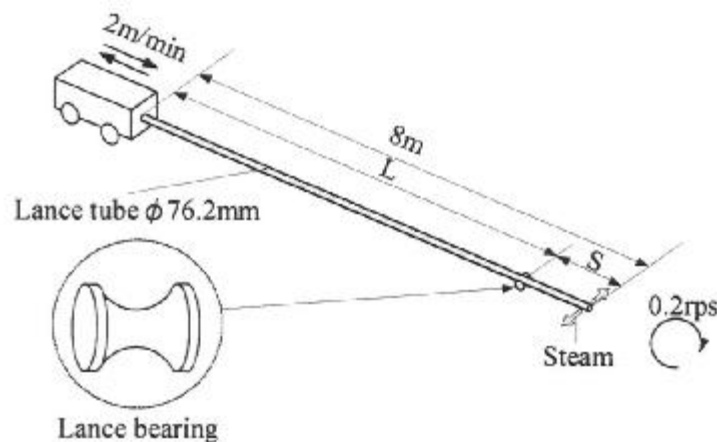
Fig.1. Schematic of a soot-blower.

From frequency analysis the observed frequencies are the eighth to the eleventh natural frequencies. Figure 2 shows the relation between the observed dominant frequencies and inserted length *S* from the support bearing to the free end of the lance. As the inserted length becomes longer, the dominant frequency

---

[*] To whom correspondence should be addressed

decreases and then increases abruptly. Since a lance bearing can rotate about the *x*-axis (Fig.1) and not about the *z*-axis, and the lance rotates about its axis parallel to the *z*-axis, the vibrations were considered to be induced by the tangential friction force between the lance and the lance bearing.
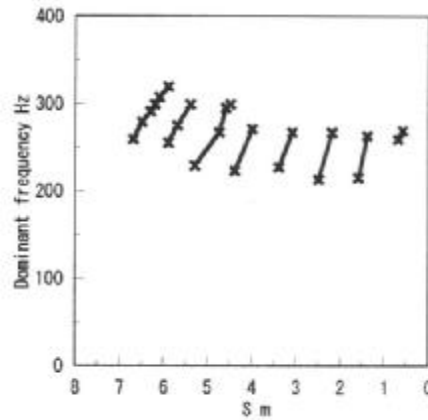
Fig.2. Observed vibration frequencies.

So far the friction induced vibration has been studied by many researches; Adams (1996) investigated self-excited oscillations in sliding, and found that the mechanism responsible for the instability is a result of the interaction of certain complex modes of vibration with the friction force of the moving springs. Rise (1983) investigated the stability of steady frictional slipping.

2. Analysis

To clarify the phenomena mentioned above we use an analytical model shown in Fig.3. Further we assume that gravitational force has little effect on the phenomena. Since a lance is very long and flexible, it is treated as a uniform circular shaft. The equations of motion are given as

$$\rho A \frac{\partial^2 u_j}{\partial t^2} + EI \frac{\partial^4 u_j}{\partial x_j^4} = 0 \,, \qquad \rho A \frac{\partial^2 w_j}{\partial t^2} + EI \frac{\partial^4 w_j}{\partial x_j^4} = 0 \,, \qquad (j = 1,2) \tag{2.1}$$

where u_j and w_j are displacements in the *y*-and *z*-direction, respectively, ρ shaft density, *A* cross section, and *EI* flexural rigidity (for example, Den Hartog (1985), Ray *et al*. (1975), Thomson (1981)). A shaft rotates at constant angular velocity ω, and is supported by a lance bearing, hereinafter called an intermediate bearing, whose stiffness is *k*. u_1 and w_1 are displacements for $0 \le x_1 \le a$; u_2 and w_2 for $-b \le x_2 \le 0$. There is a relation between the coordinates x_1 and x_2

$$x_1 + L = x_2 \,. \tag{2.2}$$

A shaft is fixed at $x = 0$ and free at $x = L(x_2 = 0)$. At the intermediate bearing ($x = a$ or $x_2 = -b$), restoring and frictional forces act on the shaft. Coulomb friction is assumed between the shaft and the bearing. Therefore, the frictional force is given by a product of the restoring force and the friction coefficient μ . The restoring force is proportional to the radial displacement and the frictional force acts tangentially. Therefore, at $x = a$ (or $x_2 = -b$)

$$-EI\frac{\partial^3 u_1(a)}{\partial x^3} + ku_1(a) + \mu kw_1(a) = -EI\frac{\partial^3 u_2(-b)}{\partial x_2^3}, \tag{2.3}$$

$$-EI\frac{\partial^3 w_1(a)}{\partial x^3} + kw_1(a) - \mu ku_1(a) = -EI\frac{\partial^3 w_2(-b)}{\partial x_2^3}, \tag{2.4}$$

and the slope and moment of the shaft are continuous.
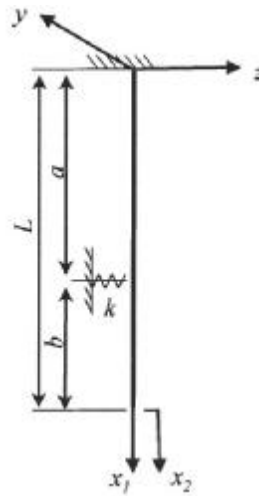
Fig.3. Analytical model.

Assuming the solutions of Eq.(2.1) as

$$u_j = U_j(x)e^{i\hat{s}t}, \qquad\qquad w_j = W_j(x)e^{i\hat{s}t}, \tag{2.5}$$

we get

$$\frac{d^4 U_j}{dx^4} - \frac{\hat{s}^2}{c_a^2}U_j(x) = 0, \qquad \frac{d^4 W_j}{dx^4} - \frac{\hat{s}^2}{c_a^2}W_j(x) = 0, \qquad (j=1,2) \tag{2.6}$$

where $\qquad i = \sqrt{-1}, \qquad c_a^2 = EI/(\rho A). \tag{2.7}$

Solutions of Eqs (2.6) are expressed as

$$U_1 = C_{11}\sin\lambda\bar{x} + C_{12}\cos\lambda\bar{x} + C_{13}\sinh\lambda\bar{x} + C_{14}\cosh\lambda\bar{x}$$

$$U_2 = C_{21}\sin\lambda\bar{x}_2 + C_{22}\cos\lambda\bar{x}_2 + C_{23}\sinh\lambda\bar{x}_2 + C_{24}\cosh\lambda\bar{x}_2$$

$$W_1 = C_{31}\sin\lambda\bar{x} + C_{32}\cos\lambda\bar{x} + C_{33}\sinh\lambda\bar{x} + C_{34}\cosh\lambda\bar{x}$$

$$W_2 = C_{41}\sin\lambda\bar{x}_2 + C_{42}\cos\lambda\bar{x}_2 + C_{43}\sinh\lambda\bar{x}_2 + C_{44}\cosh\lambda\bar{x}_2$$

(2.8)

where $\qquad \bar{x} = x/L$, $\qquad \lambda^4 = -\hat{s}^2 L^4 / c_a^2$. (2.9)

Applying the boundary conditions, we get a characteristic equation for λ as

$$\mu^2\{\cos[\alpha\lambda]\sinh[\alpha\lambda] + \cosh[\lambda - \alpha\lambda](\sin[\alpha\lambda]\cos[\lambda - \alpha\lambda]\sinh[\alpha\lambda]) - \cos[\lambda - \alpha\lambda]\sinh[\lambda - \alpha\lambda] +$$
$$- \cosh[\alpha\lambda](\cosh[\lambda - \alpha\lambda]\sin[\lambda] + \sin[\alpha\lambda] - \cos[\alpha\lambda]\cos[\lambda - \alpha\lambda]\sinh[\lambda - \alpha\lambda])\} +$$
$$+ \{2\lambda^3 + 2\lambda^3\cos[\lambda]\cosh[\lambda] - \kappa\cosh[\lambda - \alpha\lambda]\sin[\lambda - \alpha\lambda] - \kappa\cos[\alpha\lambda]\sinh[\alpha\lambda] +$$
$$- \kappa\cos[\alpha\lambda]\cos[\lambda - \alpha\lambda]\cosh[\lambda - \alpha\lambda]\sinh[\alpha\lambda] + \kappa\cos[\lambda - \alpha\lambda]\sinh[\lambda - \alpha\lambda] +$$
$$+ \kappa\cosh[\alpha\lambda](\cosh[\lambda - \alpha\lambda]\sin[\lambda] + \sin[\alpha\lambda] - \cos[\alpha\lambda]\cos[\lambda - \alpha\lambda]\sinh[\lambda - \alpha\lambda])\} = 0$$

(2.10)

where $\qquad \kappa = kL^3/EI$, $\qquad \alpha = a/L$, $\qquad \beta = b/L$. (2.11)

Equation (2.10) is solved numerically for l .
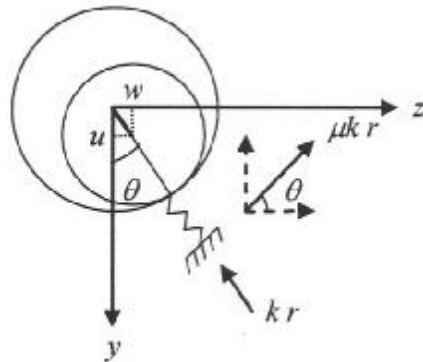
Fig.4. Restoring and frictional forces acting on a shaft at an intermediate bearing.

The dimensionless eigenvalue $\sigma = i\hat{s}L^2/c_a$ is expressed as

$$\sigma = \pm i\lambda^2 .$$

(2.12)

Generally, since σ is a complex number, we set

$$\sigma = \sigma_R + i\sigma_I .$$

(2.13)

Figure 5 shows natural frequencies σ_I when friction does not act on a shaft at the intermediate bearing, that is, $\mu = 0$. In these cases $\sigma_R = 0$. With κ, σ_I increases gradually and then rapidly, and approaches asymptotically a natural frequency of a system pinned at the intermediate bearing. Figure 6 shows the effect of α on natural frequency σ_I when $\mu = 0$ and $\kappa = 10^5$. σ_I fluctuates with α. σ_I reaches a maximum when α coincides with one of the nodes for each mode.
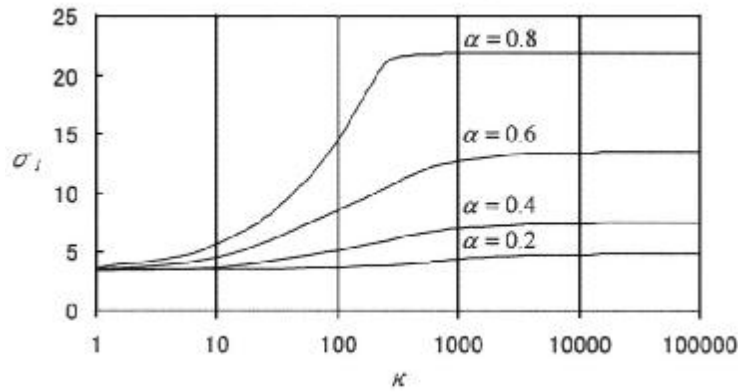
Fig.5. Effect of intermediate bearing stiffness κ or eigenvalue σ_I for various values of $\alpha (\mu = 0)$.
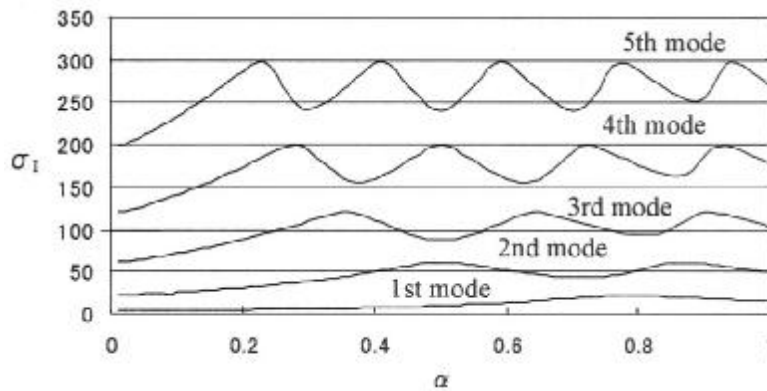
Fig.6. Effect of α on σ_I ($\mu = 0$, $\kappa = 10^5$).

Figure 7 shows dimensionless eigenvalues $\sigma = \sigma_R + i\sigma_I$ of the first mode when $\alpha = 0.5$ and $\kappa = 2000$ for three values of friction coefficient μ. For $\mu > 0$, eigenvalues σ are complex numbers. Further, the frictional force destabilizes the system since there are always two eigenvalues with positive σ_R for each mode. The absolute value of real part of σ_R, that is $|\sigma_R|$, increases with μ. The system is more unstable for larger values of μ. The shaft whirls in the opposite direction to the shaft rotation since the unstable vibration is due to frictional force acting at an intermediate bearing.
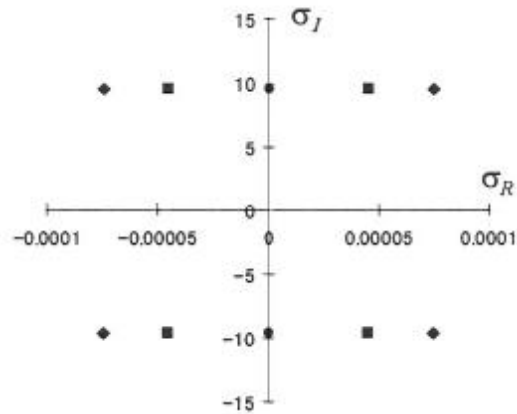
Fig.7. Eigenvalues σ ($\alpha = 0.5$, $\kappa = 2000$, • $\mu = 0$, ■ $\mu = 0.3$, ♦ $\mu = 0.5$ =0.5).

Figure 8 shows that $|\sigma_R|$ does not always decrease with the order of mode. This may imply the occurrence of vibrations of higher modes in the soot-blower described in the introduction.

a) $\alpha = 0.4$ b) $\alpha = 0.6$ c) $\alpha = 0.8$
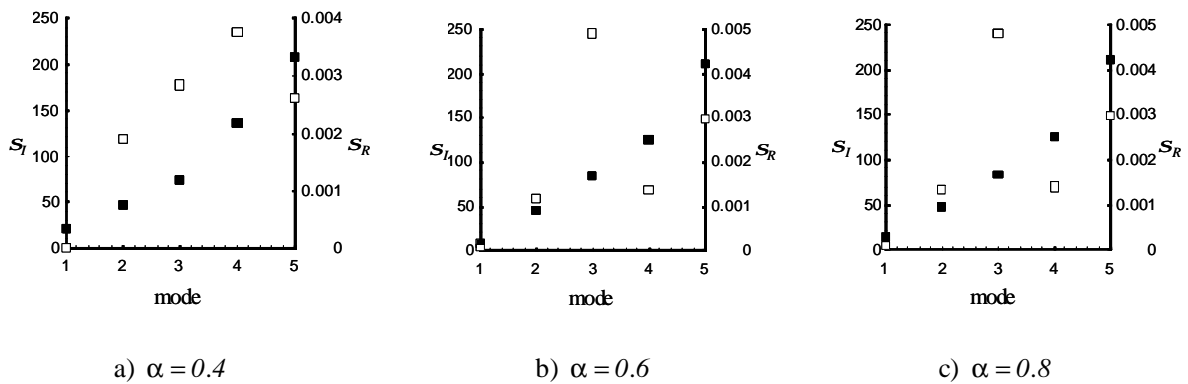
Fig.8. ■: σ_I , □: σ_R ($\kappa = 2000$, $\mu = 0.5$).

Figure 9 shows the vibration of σ_R on α and κ. We only show lager values of σ_R by circles whose diameter represent the magnitude of σ_R. We note that generelly σ_R is lager for a higher mode. σ_R increases with κ. Lager values of σ_R appear around higher values of σ_I for each mode. A large value of σ_R means that the corresponding mode is more unstable for that condition, i.e., α. In calculation, an eigen value does not depend on the shaft speed explicitly.
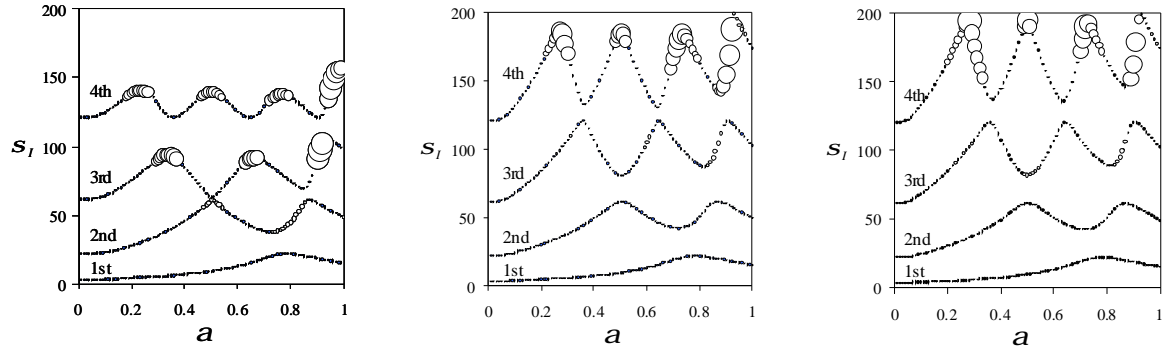
(a) $\kappa = 2000$ ($\circ: \sigma_R = 0.0061$) (b) $\kappa = 8000$ ($\circ: \sigma_R = 0.00186$) (c) $\kappa = 10000$ ($\circ: \sigma_R = 0.00128$)

Fig.9. Effect of κ to σ_I and σ_R ($\cdots\cdots: \sigma_I$; $\circ: \sigma_R$, whose diameter is proportional to magnitude of σ_R).

3. Experimental results and discussion

Figure 10 shows the experimental apparatus. The flexible shaft of *3 mm* in diameter is held by four ball bearings and a intermediate bearing, which is located at a distance $L - \alpha$ from the free and. The distance between fourth ball bearing and free end is *1720 mm.*
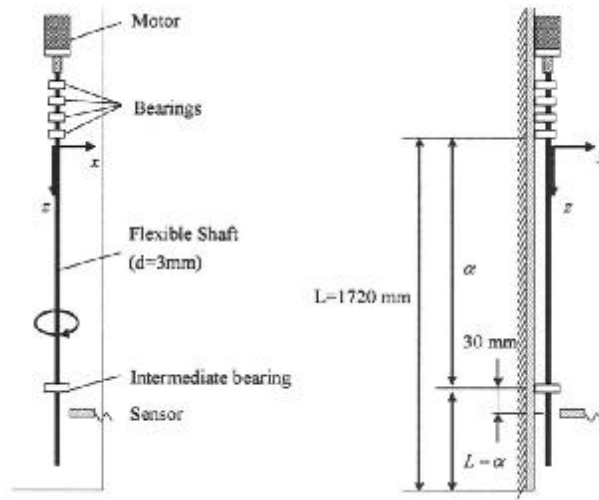
Fig.10. Experimental apparatus.

Figure 11a shows the observed frequencies σ_I for intermediate bearing position α. The diameter of a circle plotted in the figure represents the amplitude of vibration. Dotted curves in the figure are calculated damped natural frequencies, with which observed frequencies agree well. We note that large vibrations occur in a range where natural frequency increases. Figure 11b shows the calculated natural frequency σ_I versus α. A diameter of a circle in the figure represents the magnitude of σ_R. σ_R is a measure of instability. Comparing Figs 11 we note that large vibration occurs for ranges of α where σ_R is large.

(a) Experimental results   (b) Calculated results ($\circ$: $\sigma_R = 0.000044$)
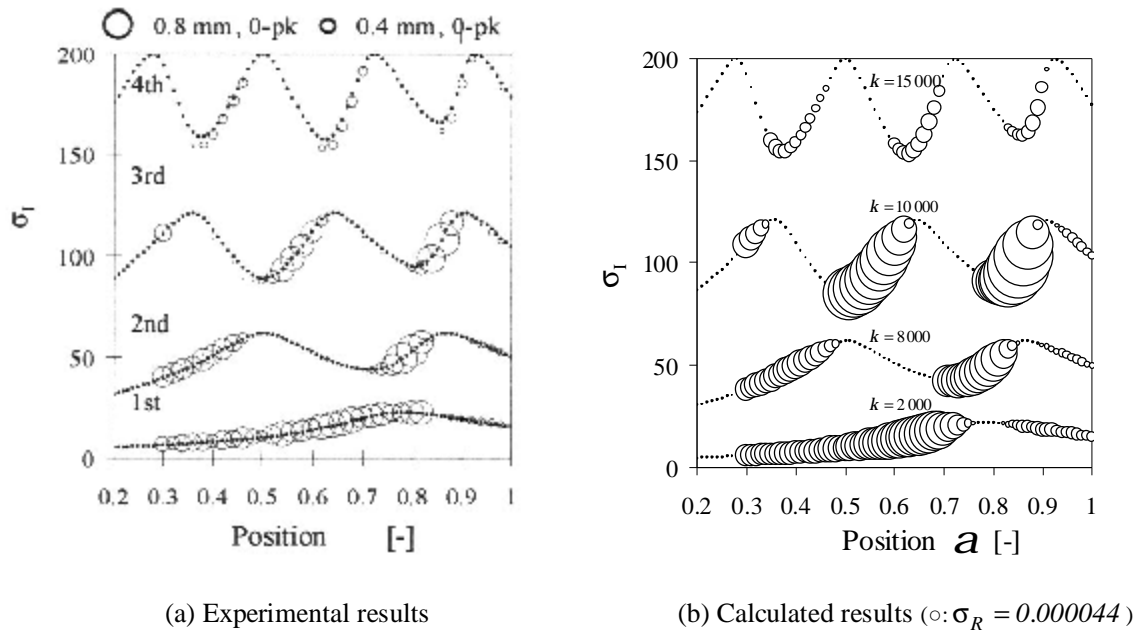
Fig.11. Observed vibrations, experimental and calculation results.

Figure 12 shows the relation between the applied force and the displacement of a rubber ring. We note that rubber stiffness increases with the displacement. Non-dimensional stiffness coefficient κ are in the range from *20 000* to *60 000*.
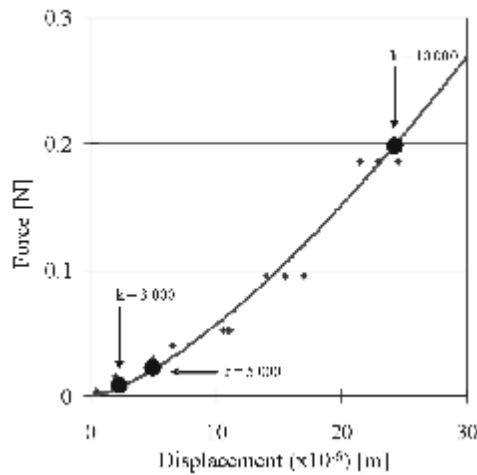
Fig.12. Measured relation between the force and the displacement of a rubber ring.

We assume that for higher speeds the displacement of a rubber ring is larger, that is, the rubber stiffness is larger. Therefore, we use different values of κ in calculation.

4. Summary

From experimental and analytical investigations, we obtain the following conclusions:
1. Analytical results show that the real part of an eigenvalue does not always increase or decrease monotonically with the order of mode. Therefore, some modes appear more prominently.
2. Since large vibration is observed in a condition where real part of an eigenvalue is large, the observed vibration is considered to be a self-excited vibration due to friction acting at an intermediate bearing.

Nomenclature

a – intermediate bearing position
c_a – see Eq.(2.7)
k – bearing stiffness
L – shaft length
$\hat{s}$ – see Eq.(2.5)
$\alpha = a/L$
$\sigma = \sigma_R + i\sigma_I = i\hat{s}L^2/c_a$ – dimensionless eigenvalue
σ_I – dimensionless eigen frequency
$\kappa = kL^3/(EI)$ – dimensionless stiffness
μ – friction coefficient

References

Adams G.G. (1996): *Self-excited oscillations in sliding with a constant friction coefficient – a simple mode.* – Trans. ASME, J. Tribology, vol.118, pp.819-823.

Den Hartog J.P. (1985): *Mechanical Vibration.* – Dover Publication.

Ray W., Clough J. and Penzien A. (1975): *Dynamics of Structures.* – McGraw-Hill.

Rise J.R. and Ruina A.L. (1983): *Stability of steady frictional slipping.* – Trans. ASME, J Applied Mechanics, vol.50, pp.343-349.

Sato Y. (2001): *Vibrations of a flexible rod induced by friction.* – Proc. ISVCS, pp.6-10.

William T. Thomson (1981): *Vibration with Applications.* – George Allen & Unwin.